Int. J. Appl. Math. Comput. Sci., 2004, Vol. 14, No. 4, 469–475

TRACKING CONTROL ALGORITHMS FOR A LABORATORY AERODYNAMICAL SYSTEM

PRZEMYSŁAW GORCZYCA*, KRYSTYN HAJDUK*

* Institute of Automatics, AGH University of Science and Technology
Al. Mickiewicza 30, 30–059 Cracow, Poland
e-mail: {przemgor, kha}@ia.agh.edu.pl

The tracking control problem of a strongly nonlinear MIMO system is presented. The system shares some features with a helicopter, such as important interactions between the vertical and horizontal motions. The dedicated I/O board allows for control, measurements and communication with a PC. The RTWT toolbox in the MATLAB environment is used to perform real-time experiments. The control task is to track a predefined reference trajectory. A mathematical model of the system, containing experimental characteristics, is used to design the controllers: a multidimensional PD, a suboptimal controller in the sense of a quadratic performance index and a variable gain controller.

Keywords: nonlinear systems, real-time control, tracking control, suboptimal controller

1. Introduction

Among autonomous flying systems, helicopters have particularly interesting dynamic features. The main difficulties in designing controllers for them follow from nonlinearities and couplings (Avila-Vilchis *et al.*, 2003; Gorczyca *et al.*, 1995; Horáček, 2000). Another problem is that the inputs are not directly applied torques or forces. The aerodynamical torques and forces steering a helicopter are created by the main and tail rotors. Many authors, both academic and industrial research workers, have dealt with helicopter control problems and modelled the system with the use of the blade element approach, blade element momentum theory and general flow theory (Avila-Vilchis *et al.*, 2003; Luo *et al.*, 2003; Murkherjee and Chen, 1993; Padfield, 1996). Often, linearized models have been used for controller design (Dudgeon *et al.*, 1997, Luo *et al.*, 2003).

The dynamics of the system considered are simpler than those of a real helicopter, but they retain the most important helicopter features such as couplings and strong nonlinearities. A 2-DOF model is considered and, unlike in most of recent works, aerodynamical forces and torques are introduced as experimentally measured characteristics. The simulation and real-time experiments in closed loop are performed and comparisons are presented. The system in question is interesting because it makes it possible to perform various experiments in the field of modelling, identification and control theory.

Figure 1 shows a laboratory model of the Twin Rotor Aerodynamical System (TRAS). At both ends of a beam,

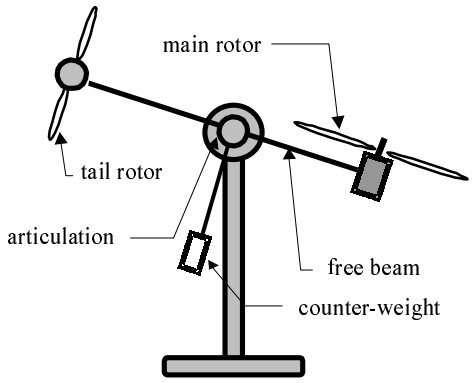

Fig. 1. Configuration of the TRAS.

joined to its base with an articulation, there are two propellers driven by DC motors. The articulated joint allows the beam to rotate so that its ends move on spherical surfaces. A counter-weight fixed to the beam determines a stable equilibrium position. The system is balanced in such a way that when the motors are switched off, the main rotor end of the beam is lowered and it stops at the position -0.5319 [rad]. The rotors are positioned perpendicularly to each other so that the movement in the vertical plane and the movement in the horizontal plane are each affected by the thrust of only one propeller. The controls of the system are the supply voltages of the motors. The measured signals are the two position angles that determine the position of the beam in space, and the angular velocities of the rotors. The positions are measured using incremental encoders, and the angular velocities of the ro-

tors are measured by tachogenerators. The angular velocities of the beam are reconstructed by a simple differentiation and a second-order filtering of the measured position angles of the beam.

It should be noted that the system has no angular velocity feedback carried out by an internal gyro control system. This introduces an additional difficulty because it brings the system near instability.

2. Mathematical Model

The mathematical model is developed under some simplifying assumptions. First, it is assumed that the dynamics of the propeller subsystem can be described by ordinary differential equations. Further, it is assumed that friction in the system suspension is of the viscous type. It is also assumed that the propeller-air subsystem can be described in accordance with the postulates of stream flow theory. These assumptions (except for the friction assumption) are widely applied in the literature (Avila-Vilchis *et al.*, 2003; Padfield, 1996). The mathematical model of the TRAS is a set of six nonlinear ordinary differential equations, being the state equations, and six algebraic output equations. The variables of the model are as follows: u is the control input, x is the state, and y is the output,

$$u = [u_1 \;\; u_2]^\top, \quad x = [x_1 \;\; x_2 \;\; x_3 \;\; x_4 \;\; x_5 \;\; x_6]^\top,$$

$$y = [y_1 \;\; y_2 \;\; y_3 \;\; y_4 \;\; y_5 \;\; y_6]^\top,$$

where u_1 is the control input for the tail rotor, ($|u_1| \leq 1$), u_2 is the control input for the main rotor ($|u_2| \leq 1$, x_1 is the angular velocity of the tail rotor [rad/s], x_2 is the horizontal angular momentum of the beam $[\mathrm{kg} \cdot \mathrm{m}^2 \cdot \mathrm{rad/s}]$, x_3 is the azimuth position of the beam [rad] ($|x_3| \leq \pi$), x_4 is the angular velocity of the main rotor [rad/s], x_5 is the pitch velocity of the beam [rad/s], x_6 is the pitch angle of the beam [rad] ($|x_6| \leq \pi/4$), y_2 is the azimuth velocity of the beam [rad/s]. The controls are dimensionless signals taking values in the interval $[-1, +1]$, which corresponds to the range $[-30\mathrm{V}, +30\mathrm{V}]$ of the input voltage controlling the DC motors. The position angles and the corresponding angular velocities of the rotors are shown in Fig. 2.

The state equations are as follows:

$$\begin{aligned}
\dot{x}_1 &= u_1 - f_h(x_1),\\
\dot{x}_2 &= (m_1 u_2 - m_2 x_4 + g_h(x_1))\cos x_6 - m_3 q(x_2, x_6),\\
\dot{x}_3 &= q(x_2, x_6),\\
\dot{x}_4 &= u_2 - f_v(x_4),\\
\dot{x}_5 &= m_4 u_1 - m_5 x_1 + g_v(x_4) - m_6 x_5 + r(x_2, x_6),\\
\dot{x}_6 &= x_5.
\end{aligned} \tag{1}$$

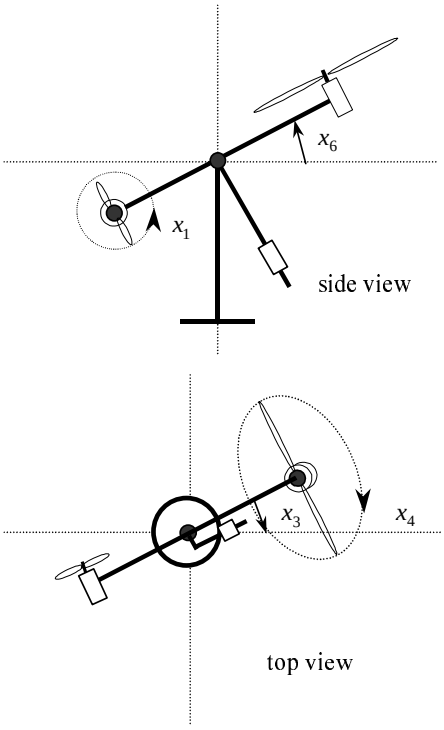

Fig. 2. Position angles and rotor velocities.

The output equations have the form

$$y_i = x_i, \;\; i = 1, 3, 4, 5, 6, \quad y_2 = q(x_2, x_6).$$

According to stream flow theory, the functions $f_h(x_1)$, $f_v(x_4)$, $g_h(x_1)$ and $g_v(x_4)$ depend, in a complex way, on the angular velocities x_1 and x_4, and on the geometry of the rotor blades. Instead of directly using relations following from that theory, aerodynamical thrusts and motion resistances were experimentally measured and the obtained data were approximated by polynomials.

The functions $f_h(x_1)$, $f_v(x_4)$, $g_h(x_1)$, $g_v(x_4)$, $r(x_2, x_6)$ and $q(x_2, x_6)$ are defined as follows:

$$\begin{aligned}
f_h(x_1) &= a_1 x_1 + a_2 x_1^2 + a_3 x_1^3 + a_5 x_1^5,\\
f_v(x_4) &= b_1 x_4 + b_2 x_4^2 + b_3 x_4^3 + b_4 x_4^4 + b_5 x_4^5,\\
g_h(x_1) &= c_1 x_1 + c_2 x_1^2 + c_3 x_1^3 + c_5 x_1^5 + c_7 x_1^7,\\
g_v(x_4) &= d_1 x_4 + d_2 x_4^2 + d_3 x_4^3 + d_4 x_4^4 + d_5 x_4^5 + d_8 x_4^8,\\
r(x_2, x_6) &= -e_1 q(x_2, x_6)^2 \sin x_6 \cos x_6 - e_2 \cos x_6\\
&\quad - e_3 \sin x_6,\\
q(x_2, x_6) &= \frac{x_2}{k_1 \cos^2 x_6 + k_2}.
\end{aligned} \tag{2}$$

The functions $f_h(x_1)$, $f_v(x_4)$, $g_h(x_1)$ and $g_v(x_4)$ represent the motion resistance and aerodynamical thrust of rotors and were determined using an electronic scale.

The functions $f_h(x_1)$ and $f_v(x_4)$ are inverses of the functions which define the dependence of the angular velocities of propellers on motor controls. These functions describe the general effect of aerodynamical drag, viscous friction of motor bearings, and the influence of the EMF induced in motors. The functions $g_h(x_1)$ and $g_v(x_4)$ determine the moments of forces, caused by the thrust of the tail and main rotors, as functions of the angular velocities of the propellers.

The function $q(x_2, x_6)$ defines the variability of the moment of inertia about the vertical axis. The function $r(x_2, x_6)$ describes the influence of the moments of forces depending on the pitch angle of the beam x_6. It is a sum of two moments: the one from the gravity forces of system elements, and the one from the centrifugal force caused by the rotational movement about a vertical axis. The forms of the functions $r(x_2, x_6)$ and $q(x_2, x_6)$ result from the system geometry.

Figure 3 shows plots of the functions $f_h(x_1)$, $g_h(x_1)$, $r(x_2, x_6)$ and $q(x_2, x_6)$. For a further application, the measured characteristics are replaced by their polynomial approximations (2). The coefficient values are given in Table 1.

Table 1. Coefficient values.

i	a_i	b_i	c_i	d_i	e_i	k_i	m_i
1	2.1681	0.5644	$12.5466{\cdot}10^4$	0.12959	1.3609	0.0474	0.0042
2	$-1.8304{\cdot}10^3$	$3.8832{\cdot}10^3$	$-3.9488{\cdot}10^4$	0.01592	2.7099	0.0079	0.0034
3	$5.8401{\cdot}10^3$	$2.7624{\cdot}10^2$	$11.3489{\cdot}10^5$	0.02077	4.6047		0.0123
4		$-6.1689{\cdot}10^4$		$-1.1990{\cdot}10^{11}$			0.0215
5	$2.4107{\cdot}10^6$	$2.1114{\cdot}10^5$	$-3.1700{\cdot}10^7$	$-1.6271{\cdot}10^4$			0.0265
6							0.0391
7			$4.9421{\cdot}10^{10}$				
8				$4.2985{\cdot}10^6$			

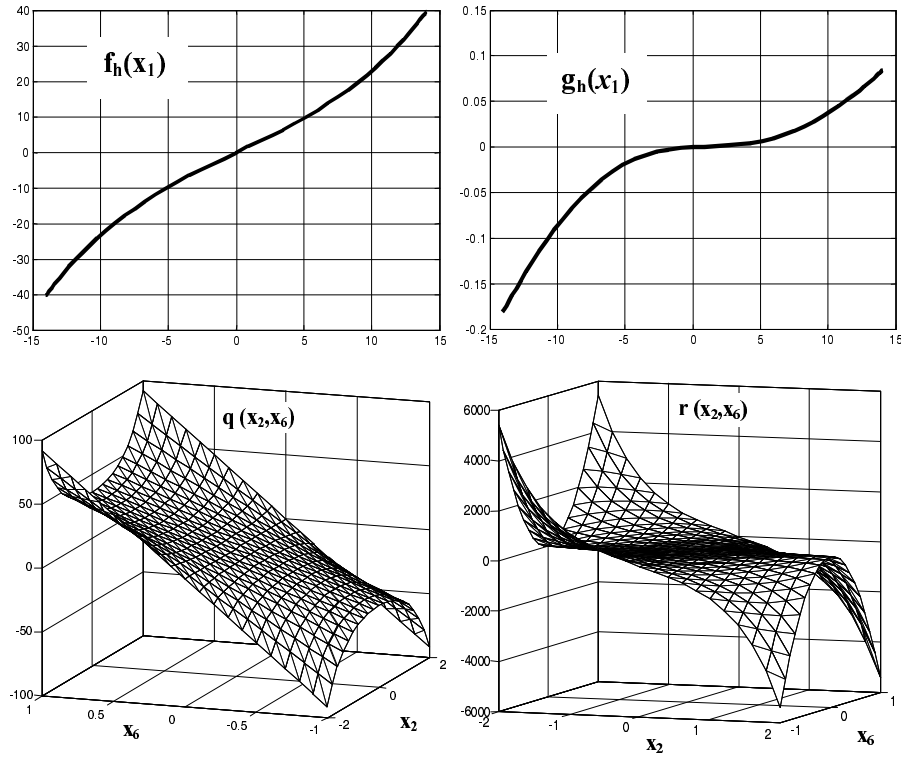

Fig. 3. Plots of the characteristics $f_h(x_1)$, $q(x_2, x_6)$, $g_h(x_1)$ and $r(x_2, x_6)$.

Figure 4 shows the Simulink model of the TRAS. The model is used to design the controllers. To keep the

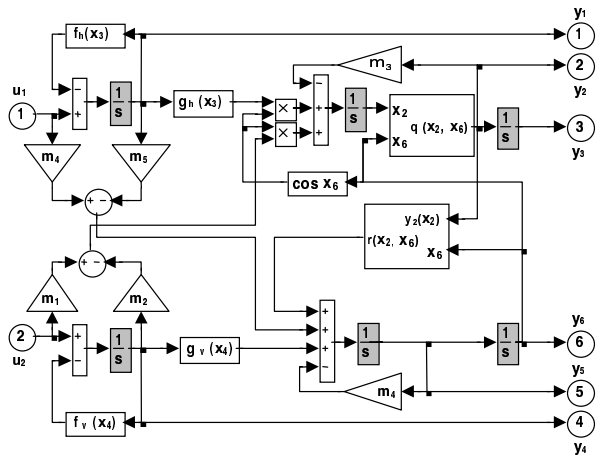

Fig. 4. Simulink model of the TRAS.

beam in a horizontal position (zero pitch), the controlling of the main rotor is needed. It results in the appearance of a torque, caused by cross-coupling, in the perpendicular axis. If we want to hold a fixed azimuth (assumed to be equal to 0), the tail rotor control is needed. The operating steady-state (pitch and azimuth equal to 0) $x_0 = [-5.1718 \;\; 0 \;\; 0 \;\; 4.371700]^\top$ is maintained by constant control $u_0 = [\; -0.28 \quad 0.677 \;]^\top$. For this control value the real TRAS is near the equilibrium state. In the real helicopter the pilot tunes the initial thrust values after the take-off (trimming). The state x_0 is not an asymptotically stable point, because in the linearized model one of the eigenvalues related to the azimuth movement is equal to 0. The state matrix A of the model linearized at the point x_0 has the form

$$A = \begin{bmatrix} -2.2203 & 0 & 0 & 0 & 0 & 0 \\ 0.0084 & -0.8909 & 0 & 0 & -0.0108 & 0 \\ 0 & 0 & 0 & 0 & 0 & 1.0000 \\ 0 & 18.0702 & 0 & 0 & 0 & 0 \\ 0 & 0 & 0 & 0 & -0.4491 & 0 \\ -0.0120 & 0 & -4.6047 & 0 & 0.1296 & -0.0391 \end{bmatrix}.$$

It has the eigenvalues $\lambda_{1,2} = -0.0196 \pm 2.1458\mathrm{i}$, $\lambda_3 = -0.8908$, $\lambda_4 = 0$, $\lambda_5 = -2.2203$, and $\lambda_6 = -0.449$. Because of that, a conventional controller is applied to keep the TRAS at the equilibrium point.

3. Control Task

The main control task is the stabilization of the system (Gorczyca and Turnau, 1998; Witkowski, 1986), which corresponds to maintaining the hover state of the real helicopter (Avila-Vilchis *et al.*, 2003). An additional control

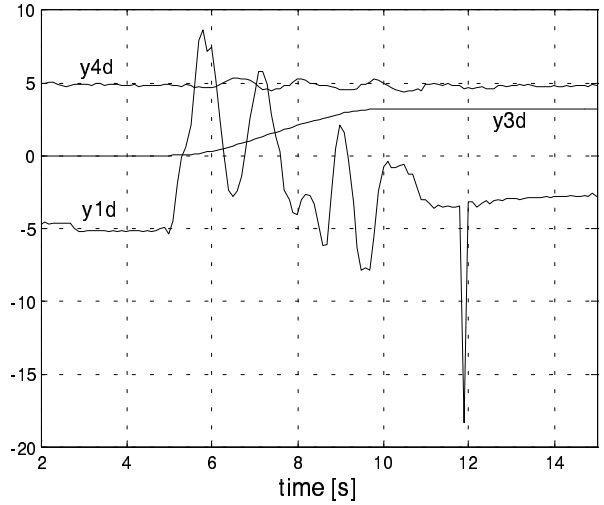

Fig. 5. Reference trajectory.

problem for the TRAS setup is to make the beam move to a specified azimuth tracking the reference trajectory presented in Fig. 5 during the manoeuver. The change in the azimuth between the initial and target states is π.

The desired azimuth is denoted by y_{3d}, the desired pitch by y_{6d}, the desired angular velocities of the main and tail rotors by y_{4d} and y_{1d}, respectively . The desired pitch y_{6d} and pitch velocity of the beam y_{5d} are assumed to equal 0.

The control goal is to steer the system (1) from the initial state $x_0 = [-5.1718 \;\; 0 \;\; 0 \;\; 4.3717 \;\; 0 \;\; 0]^\top$ to the target state $x_f = [-5.1718 \;\; 0 \;\; \pi \;\; 4.3717 \;\; 0 \;\; 0]^\top$ tracking the reference trajectory y_d.

3.1. PD Controller

A special structure of the controller is proposed for reducing interactions between the motions in both planes (see Fig. 6). The system of equations describing the TRAS is of the sixth order, but it can be naturally separated into two sets of the third order representing the horizontal and the vertical motion, respectively. Unfortunately, there is

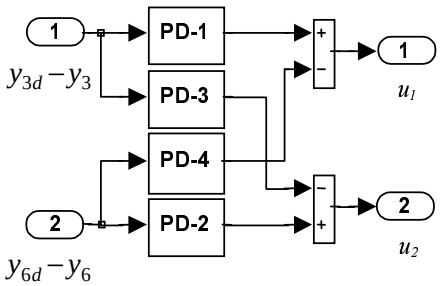

Fig. 6. Structure of the PD controller.

an important interaction between the vertical and horizontal motions. The goal of the system decoupling is to design a controller such that a change in the reference value for the pitch will cause only a vertical movement of the beam with no change in the azimuth (the beam position). A similar effect on the other axis is expected when a decoupling controller is applied. In the approach described in the sequel, the decoupling is not directly referred to, but the structure of the proposed controllers allows overcoming the complex results of interactions. For the stabilization of the TRAS at the equilibrium state, four simple PD controllers are applied.

The parameters of the PD controllers are determined by minimizing the criterion $S = \frac{1}{T}\int_0^T (e_3^2(t) + e_6^2(t))\,\mathrm{d}t$, where $e_3 = y_{3d} - y_3$ is the azimuth error and $e_6 = y_{6d} - y_6$ is the pitch error, and $T = 20\,[\mathrm{s}]$ is the time horizon. The minimizing procedure uses the simulation model of the system presented in Fig. 4. The obtained values of the parameters are $k_1 = 8.89$, $d_1 = 4.49$, $k_2 = 0.5$, $d_2 = 1$, $k_3 = 0.019$, $d_3 = 0.0004$, $k_4 = 0.0022$, $d_4 = 0.002$ (k_i stands for the coefficient of the proportional part, d_i is the coefficient of the differential part of the i-th controller).

The RTWT toolbox (MathWorks, 2004) is applied to perform real-time experiments and the RT-DAC4/PCI board is used as the interface between a PC and the TRAS setup. Figure 7 shows the Simulink model used to perform all real-time experiments described in this article. The switches allow choosing a proper controller in the experiment. The ADAPT block stands for the VGC (cf. Section 3.3) and K*inv(C) is related to the LQ optimal controller. The reference trajectory comes from the 'look-up-table' blocks.

The time responses of the closed-loop system with the PD controller are presented in Fig. 8. The quality of tracking the desired azimuth of the beam is satisfactory. The target position is reached with an error less than 1%. The control which keeps the beam motionless (for $t \le 5\,[\mathrm{s}]$ and for $t \ge 12\,[\mathrm{s}]$) is negative. This is caused by

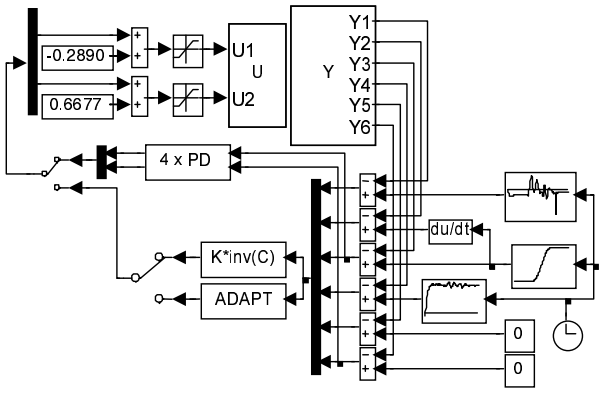

Fig. 7. Structure of the tracking control system.

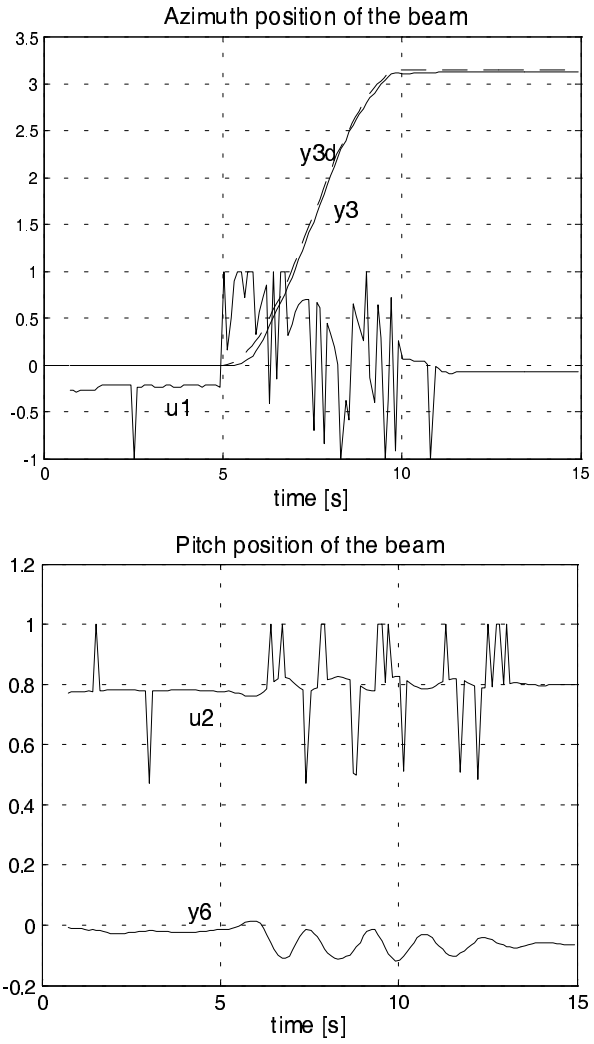

Fig. 8. Time responses of the system with the PD controller.

the angular momentum of the main rotor. The pitch of the beam oscillates with a small amplitude of 0.12 [rad] because in the vertical plane the system is of the oscillatory type with a very small damping. In some experiments (not presented here), significant sensitivity to disturbances was observed.

3.2. Suboptimal Control in the Sense of a Quadratic Performance Index

The problem is to find a control that minimizes the quadratic performance index

$$S(u) = \frac{1}{2}\int_0^\infty (\Delta y^{\mathrm{T}} Q \Delta y + \Delta u^{\mathrm{T}} R \Delta u)\,\mathrm{d}t, \qquad (3)$$

where $\Delta y = y - y_f$ and $\Delta u = u - u_0$, on the trajectories of the system (1) with the initial state x_0, target state x_f and $y_f = x_f$. Notice that the constant

control u_0 keeps the system at an arbitrary steady state with the beam in a horizontal position. As the system (1) is strongly nonlinear, the solution of the stated problem is not straightforward. If we linearize the system (1) at the point x_f, we arrive at the classical LQ problem for which the solution is known. The LQ optimal control has the form $u = -K(x - x_f) + u_0$, where the matrix K is obtained from the solution of a Riccati equation. The controller calculated in this way is suboptimal for (1) and (3). We assume that the matrices Q and R are diagonal: $Q = \mathrm{diag}(0.1,\ 0.1,\ 100,\ 100,\ 0.1,\ 0.1)$ and $R = \mathrm{diag}(3,\ 3)$. The diagonal elements of the matrices Q and R are a certain compromise between the control accuracy and cost, and assure that the controls are in the admissible range $[-1, +1]$. It should be stressed that the presented controller is optimal in the sense (3) for the linear model only.

The results of real-time experiments performed for the closed-loop system with the LQ-controller obtained for the matrices Q and R given above are shown in Fig. 9. The target azimuth is reached with a steady-state error equal to 1.97%.

3.3. Variable Gain Controller (VGC)

In this section the controller with a variable gain based on the LQ idea is presented. The gain of the controller varies along the trajectory. The design process is as follows: we split the time interval into subintervals of the length Δt each. We require that in each subinterval the system go to a point $\bar{y}_d^i$ all components which are as at the point $y_d(i\Delta t)$ situated on the reference trajectory, except the beam velocities which are assumed to be zero. This means that the point $\bar{y}_d^i$ is an equilibrum point of the system. We linearize the system at the point $\bar{y}_d^i$ and design the LQ controller minimizing the performance index (3) with $\Delta y = y - \bar{y}_d^i$ and $\Delta u = u - u_0$. For the control time equal to 15 [s] and $\Delta t = 0.1$ [s] we thus obtain a set of matrices $K_i,\ i = 1, 2, \ldots, 150$. Each of these matrices contains coefficients of the controller for the respective i-th subinterval. The control $u = -K_i(x - \bar{y}_d^i) + u_0$ is valid only in the i-th subinterval. The described algorithm is applied along the reference trajectory until the target point y_f is reached. The calculation of the matrices K_i is carried out off-line because the reference trajectory is known prior to the real time experiment. To implement the algorithm in real time, a special S-function was written. This S-function selects the appropriate matrix K_i for each subinterval.

The experimental results obtained using the VGC are presented in Fig. 10. These results are not much better than those obtained with the suboptimal controller. The steady-state error is equal to 1.94%. A comparison of the controllers considered is given in Fig. 11. The suboptimal

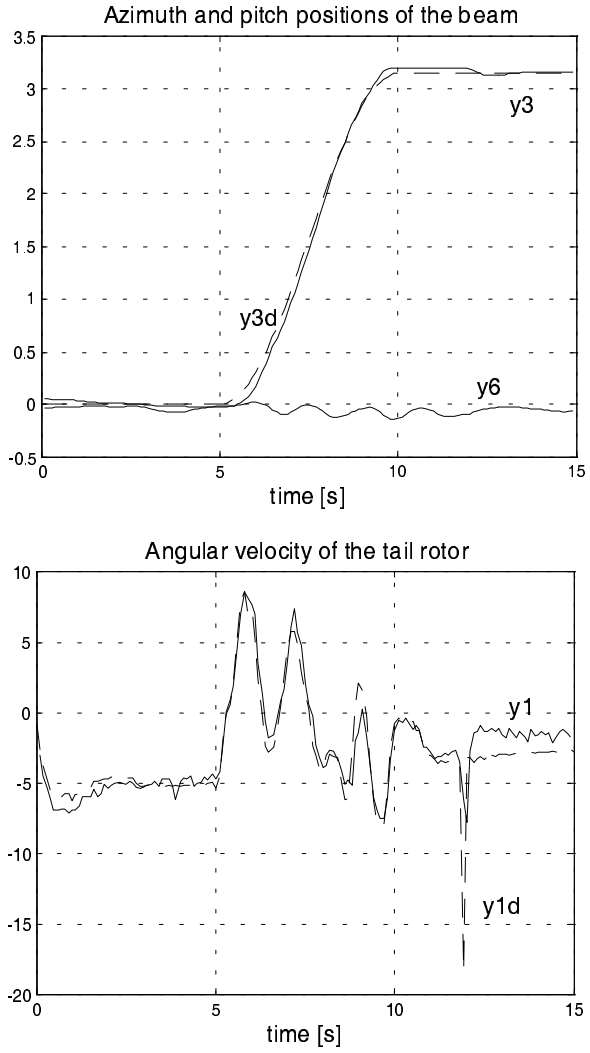

Fig. 9. Suboptimal control. The dashed line represents the reference trajectory.

controller keeps the pitch position of the beam y_6 a little better than the VGC. The quality of tracking the variable y_3, i.e., the azimuth of the beam is almost identical for both controllers. In both cases, the steady-state errors are less than 2%. It should be noted that the design of the variable gain controller requires much more calculations than that of the suboptimal one.

4. Conclusions

The presented mathematical model is sufficiently accurate to design controllers for tracking control tasks. In the case of the PD controller, the quality of tracking the reference trajectory was good, but significant sensitivity to disturbances was observed.

The suboptimal and variable gain controller were designed using the LQ methods. It appears that a very simple

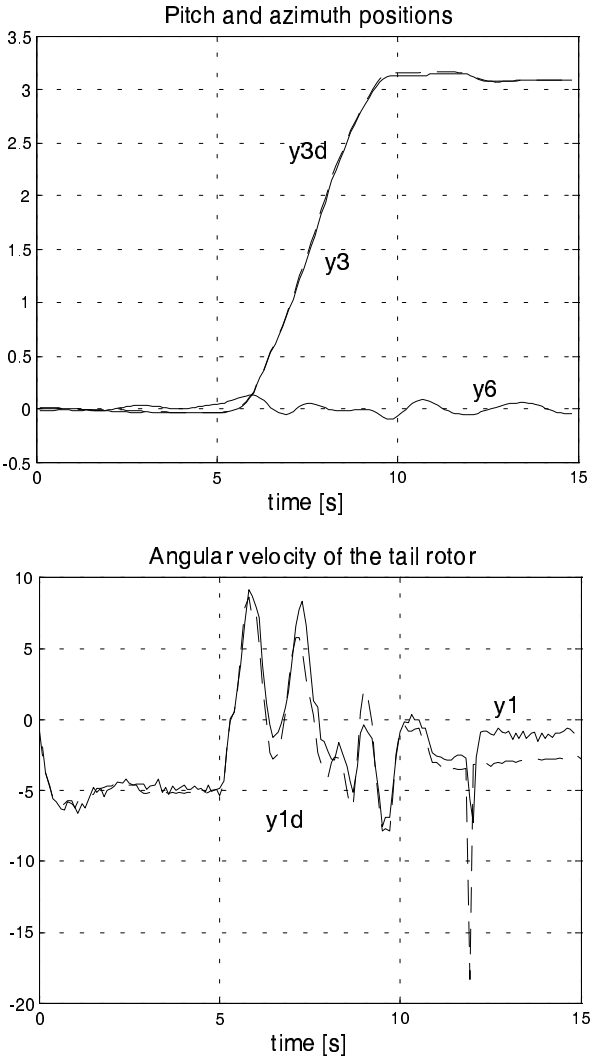

Fig. 10. Variable gain control. The dashed line represents the reference trajectory.

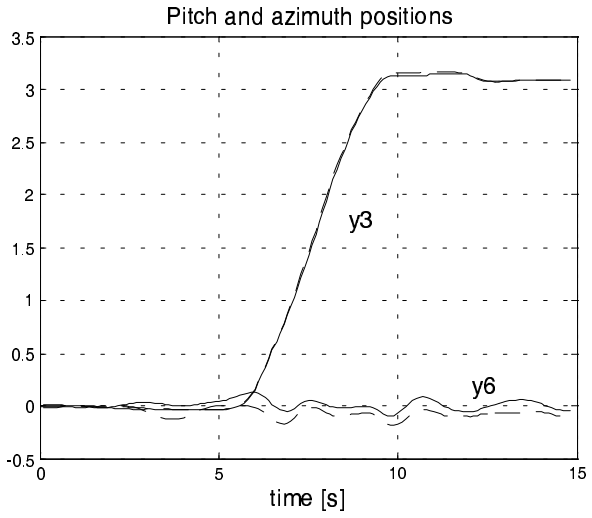

Fig. 11. Comparison of control results (suboptimal control – dashed, VGC – solid.

suboptimal controller, based on linearization at the target point only, gives results no worse than the controller with variable gain. It could be interesting to study a controller based on the idea of neighbouring trajectories (Pauluk, 2002).

The polynomial approximations of the experimentally measured aerodynamical forces and torques ensured an adequate quality of the mathematical model without using the functional relationships following from stream flow theory.

References

Avila-Vilchis J.C., Brogliato B., Dzul A. and Lozano R. (2003): *Nonlinear modeling and control of helicopters*. — Automatica, Vol. 39, No. 9, pp. 1583–1596.

Dudgeon G.J.W., Gribble J.J. and O'Reilly J. (1997): *Individual channel analysis and helicopter flight control in moderate- and large-amplitude maneuvers*. — Contr. Eng. Pract., Vol. 5, No. 1, pp. 33–38.

Gorczyca P., Hajduk K. and Kołek K. (1995): *Data acquisition and control of nonlinear multidimensional system using Matlab*. — Proc. 1st *Nat. Conf. Matlab Users*, Cracow, Poland, pp. 231–235, (in Polish).

Gorczyca P. and Turnau A. (1998): *Multidimensional nonlinear MIMO system*, In: Computer Aided Calculations (M. Szymkat, Ed.). — Cracow: CCATIE, pp. 37–60, (in Polish).

Horáček P. (2000): *Laboratory experiments for control theory courses: A survey*. — Ann. Rev. Contr., Vol. 24, No. 1, pp. 151–162.

Luo C.-C., Liu R.-F., Yang C.-D. and Chang Y.-H. (2003): *Helicopter H_∞ control design with robust flying quality*. — Aerospace Sci. Technol., Vol. 7, No. 2, pp. 159–169.

MathWorks Inc. (1994–2004): *Real-Time Windows Target – User's Guide*. — Natick : The MathWorks Inc.

Murkherjee R. and Chen D. (1993): *Control of free-flying underactuated space manipulators to equilibrum manifolds*. — IEEE Trans. Automat. Contr., Vol. 9, No. 5, pp. 561–570.

Pauluk M. (2002): *Robust control of 3D crane*. — Proc. IEEE Int. Conf. *Math. Methods in Automation and Robotics*, Szczecin, Poland, pp. 355–360.

Padfield G.G. (1996): *Helicopter Flight Dynamics: The Theory and Application of Flying Qualities and Simulation Modeling*. — Washington: AIAA.

Witkowski R. (1986): *Construction and Pilotage of Choppers*. Warsaw: WKiŁ, (in Polish).